ELECTRIC POWER
RESEARCH INSTITUTE

Recovery of Irradiation Damage by Post-Irradiation Thermal Annealing

Relevance to Hydrogen Solubility and Dry Storage Issues

WARNING:
Please read the Export Control Agreement on the back cover.

Technical Report

Recovery of Irradiation Damage by Post-Irradiation Thermal Annealing

Relevance to Hydrogen Solubility and Dry Storage Issues

1013446

Final Report, June 2006

EPRI Project Manager
A. Machiels

ELECTRIC POWER RESEARCH INSTITUTE
3420 Hillview Avenue, Palo Alto, California 94304-1395 • PO Box 10412, Palo Alto, California 94303-0813 • USA
800.313.3774 • 650.855.2121 • askepri@epri.com • www.epri.com

DISCLAIMER OF WARRANTIES AND LIMITATION OF LIABILITIES

THIS DOCUMENT WAS PREPARED BY THE ORGANIZATION(S) NAMED BELOW AS AN ACCOUNT OF WORK SPONSORED OR COSPONSORED BY THE ELECTRIC POWER RESEARCH INSTITUTE, INC. (EPRI). NEITHER EPRI, ANY MEMBER OF EPRI, ANY COSPONSOR, THE ORGANIZATION(S) BELOW, NOR ANY PERSON ACTING ON BEHALF OF ANY OF THEM:

(A) MAKES ANY WARRANTY OR REPRESENTATION WHATSOEVER, EXPRESS OR IMPLIED, (I) WITH RESPECT TO THE USE OF ANY INFORMATION, APPARATUS, METHOD, PROCESS, OR SIMILAR ITEM DISCLOSED IN THIS DOCUMENT, INCLUDING MERCHANTABILITY AND FITNESS FOR A PARTICULAR PURPOSE, OR (II) THAT SUCH USE DOES NOT INFRINGE ON OR INTERFERE WITH PRIVATELY OWNED RIGHTS, INCLUDING ANY PARTY'S INTELLECTUAL PROPERTY, OR (III) THAT THIS DOCUMENT IS SUITABLE TO ANY PARTICULAR USER'S CIRCUMSTANCE; OR

(B) ASSUMES RESPONSIBILITY FOR ANY DAMAGES OR OTHER LIABILITY WHATSOEVER (INCLUDING ANY CONSEQUENTIAL DAMAGES, EVEN IF EPRI OR ANY EPRI REPRESENTATIVE HAS BEEN ADVISED OF THE POSSIBILITY OF SUCH DAMAGES) RESULTING FROM YOUR SELECTION OR USE OF THIS DOCUMENT OR ANY INFORMATION, APPARATUS, METHOD, PROCESS, OR SIMILAR ITEM DISCLOSED IN THIS DOCUMENT.

ORGANIZATION(S) THAT PREPARED THIS DOCUMENT

Zircology Plus

NOTE

For further information about EPRI, call the EPRI Customer Assistance Center at 800.313.3774 or e-mail askepri@epri.com.

CITATIONS

This report was prepared by

Zircology Plus
36848 Montecito Drive
Fremont, CA 94536

Principal Investigator
R. Adamson

This report describes research sponsored by the Electric Power Research Institute (EPRI).

The report is a corporate document that should be cited in the literature in the following manner:

Recovery of Irradiation Damage by Post-Irradiation Thermal Annealing: Relevance to Hydrogen Solubility and Dry Storage Issues. EPRI, Palo Alto, CA: 2006. 1013446.

REPORT SUMMARY

This report provides a summary of the effects of irradiation damage annealing on phenomena important to the behavior of zirconium alloys during interim dry storage and transportation of spent fuel under inert atmospheric conditions. In particular, the report addresses annealing-effect details connected in some way with hydride re-orientation under conditions relevant to the transportation and storage phases of spent fuel.

Background

A relevant issue in the evaluation of spent fuel cladding integrity during storage and transportation is the effect of hydrides on cladding resistance to failure. At issue are the consequences of loading challenges such as accidental impact during handling, cask tip-over, or accidental drop during transportation. The degree to which spent fuel cladding, after a number of years in dry storage, could retain sufficient strength and ductility to resist catastrophic failures under these loading challenges will strongly depend on the spatial distribution and orientation of the hydrides.

Objectives

To assess the possible synergy among irradiation damage annealing, hydrogen solubility, and hydride reorientation phenomena in zirconium-based claddings.

Approach

The research team performed a literature review of the irradiation-enhanced solubility of hydrogen in zirconium-based alloys and briefly described the effects of irradiation on the microstructure of these alloys, including <a> loops, <c> loops, second-phase precipitate amorphization and dissolution. The team then reviewed the literature of post-irradiation annealing of radiation damage such as <a> loops, <c> loops, and solute re-precipitation. They followed this summary with a discussion of the potential synergy among annealing damage, hydrogen solubility, and hydride re-orientation phenomena.

Results

It is likely that hydrogen atoms interact with irradiation-produced <a> and <c> dislocation loops and/or with Fe or Cr “solutes” driven from second-phase precipitates during irradiation. The hydrogen solubility data of both McMinn et al. and Vizcaino et al. indicate that release of trapped hydrogen occurs in the temperature ranges where irradiation damage is also recovering (annealing). The “trapped” hydrogen cannot be classified as either “soluble hydrogen” or “hydrides” at any particular temperature, and it can be released to the matrix only when trapping defects are eliminated by thermal annealing. With currently available data, however, it is not possible to firmly associate the hydrogen trapping to specific defects.

Hydrogen trapping can be beneficial if it limits the amount of hydrogen going back into solution when cladding temperatures increase upon transfer of spent fuel from wet to dry storage. This would be the case when the fraction of hydrogen in the form of hydrides is lower than that needed to achieve the solubility limit given by the terminal solid solubility curve related to hydride dissolution. However, depending on the cladding thermal history during dry storage, trapped hydrogen could also be incrementally released to the zirconium matrix by thermal annealing. Such a time-delayed release of hydrogen could potentially result in enhanced precipitation of radially oriented hydrides, which is an undesirable outcome.

EPRI Perspective

In the process of responding to the Nuclear Regulatory Commission’s Requests for Additional Information during technical exchanges related to NRC Interim Staff Guidance 11, EPRI sponsored the development of a model for predicting the formation of radial hydrides under conditions typical of interim dry storage scenarios (EPRI Report 1009276). The present report is intended to qualitatively assess the impact of the enhanced solubility of hydrogen due to the formation of irradiation defects capable of trapping a fraction of the hydrogen in zirconium-based alloys. Hydrogen trapping can mitigate or potentially enhance hydride re-orientation depending on the initial magnitudes and time histories of cladding temperature and hoop stress during dry storage.

Keywords

Zirconium-based alloys
Hydrogen solubility
Irradiation damage
Thermal annealing
Hydride re-orientation

CONTENTS

LIST OF FIGURES

LIST OF TABLES

1

INTRODUCTION AND GOAL

This report provides a summary of the effects of “irradiation damage annealing” on phenomena important to the behavior of zirconium alloys during interim dry storage and transportation of spent fuel maintained in an inert atmosphere. Particularly, the report addresses annealing-effect details connected in some way with potential hydride re-orientation under conditions relevant to the transportation and storage phases of spent fuel.

A more specific description of two dry transportation/storage scenarios is given here [Machiels, 2006]:

- The “French” scenario consists in shipping spent fuel in a nitrogen atmosphere after a fairly short cooling time[1] in fuel pools located at the power plant. Shipping durations are typically 10 to 30 days during which peak cladding temperatures can be as high as 420 to 470°C. This is followed by wet storage upon arrival of the spent fuel at the reprocessing facility. After about five years following arrival at the reprocessing facility, the spent uranium oxide fuel is reprocessed. Presently, the spent MOX fuel is envisioned to be transferred into a dry storage system filled with helium after additional years of wet storage. Initial peak cladding temperatures for spent MOX fuel in dry storage have been proposed to be limited to 380°C.
- The “US” scenario consists in placing the spent fuel into large-capacity dry storage systems filled with helium at the reactor sites typically after long cooling times (5-20 years) in wet storage. Initial peak cladding temperatures are limited to 400°C [NRC, 2003]. For PWR fuels, a maximum hoop stress of ~150 MPa is generally assumed. Initially assuming peak cladding temperatures of ~400°C, these decay to ~300°C after 10 years and to ~200°C after 50 years of dry storage. Shipping is not likely to occur until a final repository or a centralized interim storage facility becomes operational.

During the transportation and storage phases, it is possible that a fraction of the hydrides present in the cladding will reorient into a radial direction from a predominantly tangential (circumferential) direction through classic hydride dissolution/reprecipitation processes. Reorientation is driven by the hoop stress/temperature/time conditions, by the amount of hydrogen present to partake in the reorientation, by the texture of the material, by the density of circumferential hydrides present in the original material, by the yield stress of the zirconium matrix, etc.

Irradiation plays a role through its effect on the matrix strength and by the possible increase in hydrogen solubility due to irradiation-driven processes, including possible trapping of hydrogen

---

[1] Typically, less than a couple of years for spent uranium oxide fuel, and somewhat longer for spent mixed oxide (MOX) fuel.

by dislocation loops or solute complexes. Irradiation damage annealing is important through its role in reducing the yield stress and by possible release of the trapped hydrogen at a time when radial hydrides can form.

This report:

1. Reviews the literature of irradiation-enhanced solubility of hydrogen (pertinent points only)
2. Gives a brief description of irradiation effects on the microstructure of Zircaloys [<a> loops, <c> loops, second-phase particle (SPP) dissolution]
3. Reviews the literature of post-irradiation annealing of radiation damage (<a> loops, <c> loops, solute re-precipitation)
4. Provides a brief summary of possible synergy among damage annealing, hydrogen solubility, and hydride reorientation phenomena
5. Suggests experiments that might be conducted to gather needed data.

2

EFFECT OF IRRADIATION ON SOLUBILITY OF HYDROGEN

Using differential scanning calorimetry (DSC) techniques, two studies have recently provided data on the effect of irradiation on the solubility of hydrogen in recrystallized (RXA) or stress relief annealed (SRA) Zircaloy-4 [McMinn et al., 2000] and in RXA Zircaloy-4 [Vizcaino et al., 2002]. Both obtained reasonable results for hydrogen solubility in unirradiated material, e.g., 200-250 ppm at 400°C (673K); 55-70 ppm at 300°C (513K). And both gave firm evidence that the apparent solubility of hydrogen is increased by irradiation. The effect of incremental fluence was ambiguous; however, it does appear that the effect on solubility increases with increasing fluence in the range 1-10 x 10^{21} n/cm^2 (E > 1 MeV) for irradiation temperatures near 300°C (573K).

McMinn et al. give an apparent solubility increase of about 25 ppm at 6-10 x 10^{21} n/cm^2 (E > 1 MeV). Vizcaino et al. indicate an apparent increase of 100-200 ppm at 9 x 10^{21} n/cm^2 (E > 1 MeV). Follow-up work by Vizcaino et al., 2005 using X-ray diffraction at room temperature, indicates >40-80 ppm of hydrogen is trapped by irradiation for material (same as earlier study) containing 180 ppm of hydrogen. It should be noted that "increase in solubility" really means increase in apparent solubility, as more than one mechanism is likely operating.

Of particular importance is that the irradiation-induced solubility increase can be largely eliminated by suitable post-irradiation thermal anneals, which cause the hydrogen to be released, or "recovered," from complex irradiation-induced defects. In the McMinn et al. study, for material having a relatively low fluence (< 5 x 10^{21} n/cm^2), partial recovery was obtained at 400°C (673K) after one hour, and full recovery at 500°C (773K) after one hour. For high fluence material (1 x 10^{22} n/cm^2), only 60% recovery was obtained at 500°C after one hour.

In the Vizcaino et al., 2002 study, the recovery results were varied. Some recovery was observed at <380°C (653K) after 10 minutes[2] in most materials. Table 2-1 gives some data, extracted from the paper. It appears that at low fluence (< 5 x 10^{21} n/cm^2, E > 1 MeV), annealing in the range 500-611°C (773-884K) releases most of the trapped hydrogen. For high fluence material (> 5 x 10^{21} n/cm^2, E > 1 MeV), annealing in the 500-611°C (773-884K) range releases only part of the trapped hydrogen.

From the data contained in Table 2-1, it is concluded that hydrogen can exist in three forms in irradiated Zircaloy: (1) as soluble hydrogen, (2) as hydrides, and (3) as hydrogen trapped by complex irradiation-produced defects. The latter can be released by post-irradiation annealing. These phenomena are related to formation and annealing of radiation damage of various types.

---

[2] It is assumed that one data "run" results in the specimen being heated for 10 minutes at 380°C (653K).

Table 2-1
Post-irradiation annealing recovery, extracted from data of Vizcaino et al., 2002

Fluence n/cm^2, E > 1 MeV	Temperature °C	Time hr	Recovery %	<c> Loops?
<5 x 10^{20}	380	0.5 – 1.3	25	No
	611	2	82	
4 x 10^{21}	380	1-32	53	Maybe
	611	83	98	
	700	1	100	
4 x 10^{21}	380	1	67	Maybe
	380	2	83	
	508	2	83	
7 x 10^{21}	611	45	68	Yes
	611	80	76	
9 x 10^{21}	380	0.7	20	Yes
	508	2	42	

Possible trapping sites for hydrogen include:

- Line dislocations – It has been demonstrated by Roy, 1965, using tritium autoradiography, that hydrogen can be trapped at deformation-induced dislocations.
- Irradiation-induced loops – For years, transmission electron microscopists have noted in anecdotal fashion that irradiated zirconium alloys behaved differently than unirradiated ones when it came to formation of hydride artifacts during observation in a transmission electron microscope (TEM). Hydrides formed easily at the surface of unirradiated TEM specimens, due to hydrogen from breakdown of hydrocarbons in the electron beam of the TEM, but not on irradiated specimens. It was conjectured that individual hydrogen atoms were "absorbed" by the dislocation loops and therefore did not form visible hydrides. Lewis, 1984 came to a more scientific conclusion, using a nuclear microanalysis technique to show that hydrogen (deuterium) was trapped in irradiation-produced defects. The trap depth was measured at 0.3 eV, which is larger than the approximately 0.1-eV depth of a line dislocation trap. In a post-irradiation condition, the number of point defects (vacancies) available for trapping is relatively small, so it is speculated that loops are the probable traps.
- Second-phase precipitates (SPPs) and solutes – It has been reported [Shalliel et al., 1997] that SPPs, such as the laves-phase SPPs, $Zr(Fe_x,Cr_{1-x})_2$, have a tendency to absorb hydrogen, and that this tendency changes as the value of *x* changes, such as during neutron irradiation in the appropriate Zr alloys. So it is possible that hydrogen could be released during annealing processes that alter the SPP chemistry. Whether or not hydrogen can be associated with the rapid-diffusing Fe or slow-diffusing Cr "solutes" as the SPP dissolves during irradiation is speculative. However, it would not be surprising for some interaction to occur since the Fe

and Cr in “solution” are in a highly unstable thermodynamic state during and after irradiation since their concentrations greatly exceed their normal solubility.

- More unknown defects – It has been shown that hydrides in Zircaloy cause a substantial dimensional change [King et al., 2002]. And it has been noted [in proprietary reports] that the observed changes cannot be accounted for by the known volumetric expansions due to hydrides. It is speculated, again, that hydrides and/or hydrogen interact with the dynamics of point defect migration or loop formation and growth to cause an increase in irradiation growth.

3

IRRADIATION DAMAGE IN ZIRCALOY ALLOYS

3.1 Dislocation Loop Geometry

An important type of defect, particularly for irradiated materials, is the dislocation loop. If a significant number of vacancies or interstitials condense on a particular plane, a disk is formed with its boundary defined by a (circular) edge dislocation. This is illustrated in Figures 3-1 and 3-2 [Franklin et al., 1983]. The Burgers vector b is perpendicular to the plane of the loop, and, therefore, is the normal to the plane on which the loop lies.

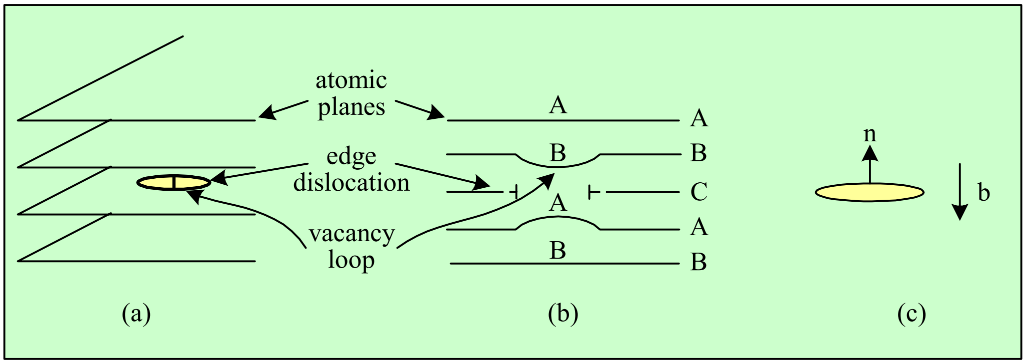

Figure 3-1
Vacancy loop, modified figure according to Franklin et al., 1983. (a) Oblique view of a vacancy loop appearing as a disk on an atomic plane; (b) side view showing the change in stacking sequence through the loop; (c) orientation of the loop normal $\vec{n}$ to the Burgers vector $\vec{b}$.

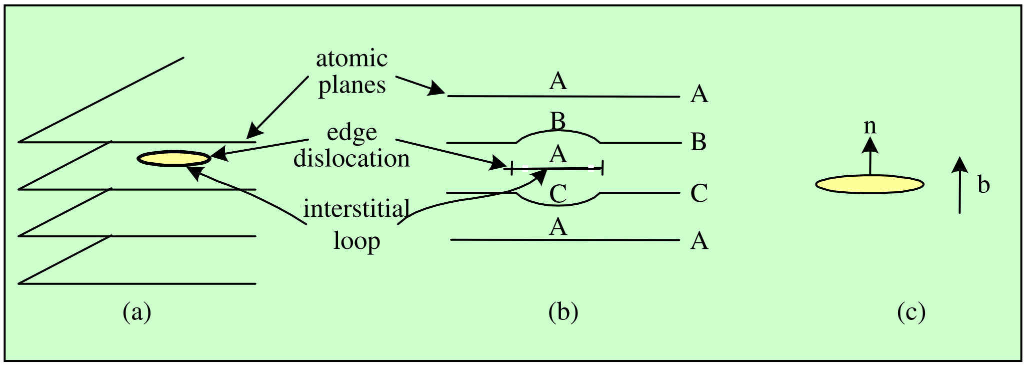

Figure 3-2
Interstitial loop, modified figure according to Franklin et al., 1983. (a) Oblique view of a interstitial loop as a disk of atoms between atomic planes; (b) side view showing the change in stacking sequence; (c) orientation of the loop normal $\vec{n}$ to the Burgers vector $\vec{b}$.

3.2 Irradiation-Produced Dislocation Loops

In structural materials like Zircaloy, the overwhelming majority of defects are caused by neutrons, and the most important type of defect is the dislocation loop. Two types of loops predominate: <a> and <c> loops. The <a> loop lies on a prism plane and has a Burgers vector in the a-direction of the HCP lattice. Table 3-1 lists some important characteristics. Both vacancy and interstitial loops exist, but more than half have vacancy character. They are very small (10-nm "black spots"), and, even in the transmission electron microscope (TEM), are difficult to analyze, Figure 3-3, where the material has been annealed to increase the loop visibility.

Table 3-1
Radiation damage, <a> loops in Zircaloy

Nature	Vacancy (excess), interstitial
Size	8 – 20 nm (80 - 200 Å)
Density	8 x 10^{14} m^{-2}
Saturation Fluence	1 x 10^{21} n/cm^2 (E > 1 MeV)
Thermal Stability	To ~400°C (673K)
Effects	Strength, ductility, growth, H solubility?

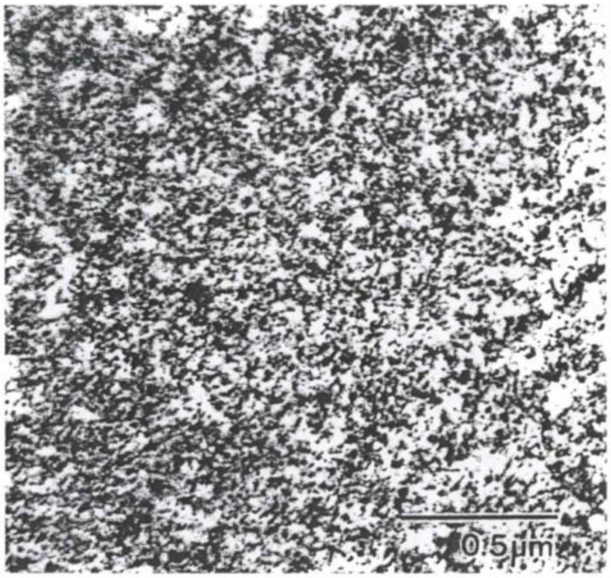

<a> type dislocation loops in neutron irradiated Zircaloy-2
after post-irradiation annealing at 723K for 1 hour .

Figure 3-3
<a> type dislocation loops in neutron-irradiated Zircaloy-2 after post-irradiation annealing at 723K for 1 hour

<a> loops form early in the irradiation and the number density reaches a saturation value at a fuel burnup less than 5 GWd/MT. The size of the loops increases with irradiation temperature, and the loops become unstable (start to disappear) at about 673K (400˚C). They have a strong effect on mechanical properties, as will be discussed later.

The <c> type of loop lies on the basal plane and has its Burgers vector, or at least a strong component of it, in the c-direction of the HCP cell. As indicated in Table 3-2, unlike the <a> loop, it is strictly a vacancy-type loop, is relatively large (100 nm), and does not form until considerable irradiation effects have occurred. In Zircaloy, <c> loops are first observed by TEM at a burnup of around 3 x 10^{21} n/cm^2 (15 GWd/MT) and increase in density the rest of the fuel lifetime. They are thermally stable to high temperature > 560°C (833K). <c> loops are thought to strongly influence irradiation growth and irradiation creep behavior, and probably do not affect mechanical properties. Figure 3-4 shows TEM images of a high density of <c> loops in highly irradiated Zircaloy. In order to "see" these loops in the TEM, they must be viewed on edge; thus they appear as straight lines in the TEM image. Such <c> loops do not appear to form readily in all zirconium alloys, particularly in those having additions of Nb or Nb and Fe [Shishov et al., 2002].

Table 3-2
Radiation damage, <c> loops in Zircaloy

Nature	Vacancy
Size	> 100 nm (1000 Å)
Density	0.5 x 10^{14} m^{-2} (For Figure 3-4)
Incubation Fluence	3 x 10^{21} n/cm^2 (E > 1 MeV)
Thermal Stability	Stable to > 560°C (833K) Form at > 200°C (475K)
Effects	Growth, creep, H solubility?

As outlined in Tables 3-1 and 3-2, the kinetics of formation of <a> and <c> type loops differ. The density of <a> type dislocation builds up quickly and saturates at a fluence less than 1 x 10^{21} n/cm^2 (E > 1 MeV), as illustrated in Figure 3-5. It appears that a fluence-incubation period exists before <c> type loops begin to form at about 3 x 10^{21} n/cm^2 (E > 1 MeV) for typical reactor temperatures, as illustrated in Figure 3-6.

For a straightforward review of the relation between irradiation-induced microstructure and Zircaloy properties, see Adamson, 2000, where more technical details and references can be found.

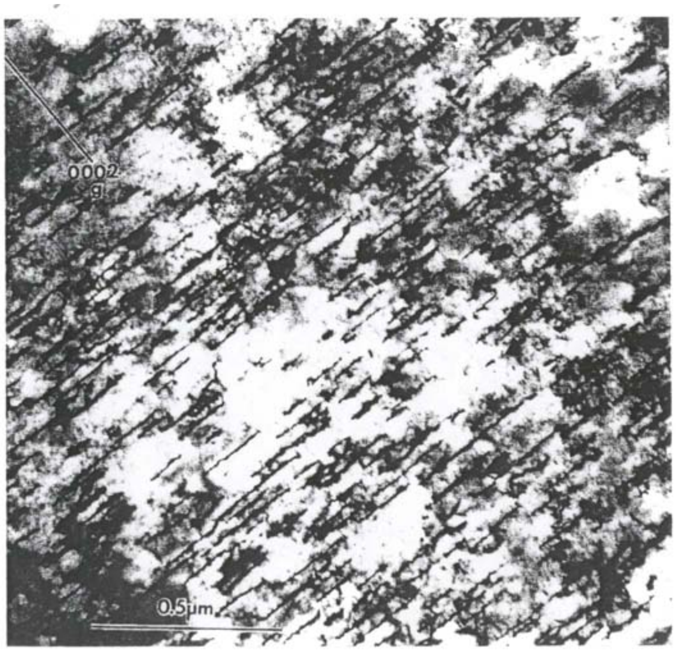

<c> type dislocations in Zircaloy-4 after a fluence of 12 x 10^{25} n/m^2 at 561K

Figure 3-4
<c> type dislocations in Zircaloy-4 after a fluence of 12 x 10^{21} n/cm^2 at 288°C (561K)

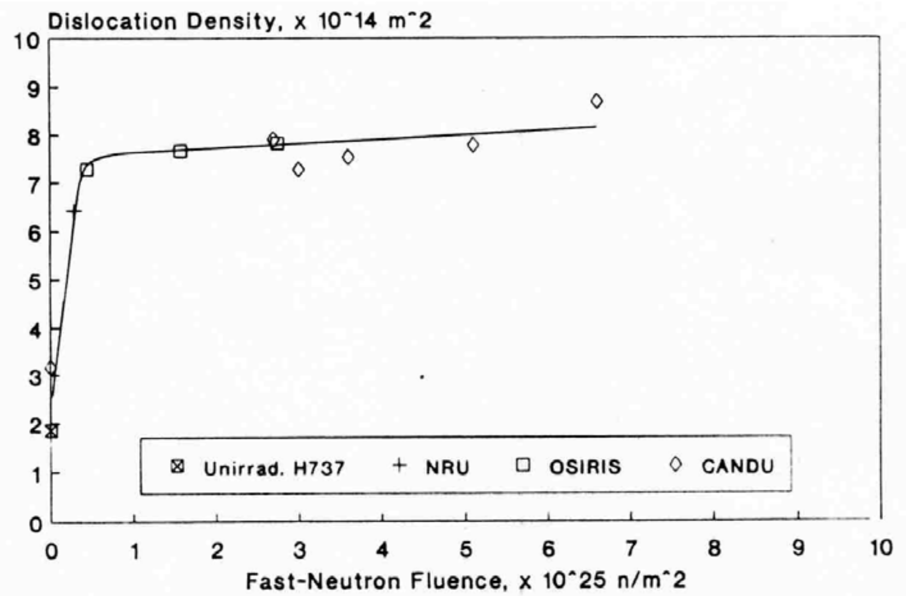

Figure 3-5
Variation of <a> type dislocation loop density x 10^{10} cm^{-2} as a function of fluence x 10^{21} n/cm^2 in various reactors at 250-290°C (523-563K) [Davies et al., 1994]

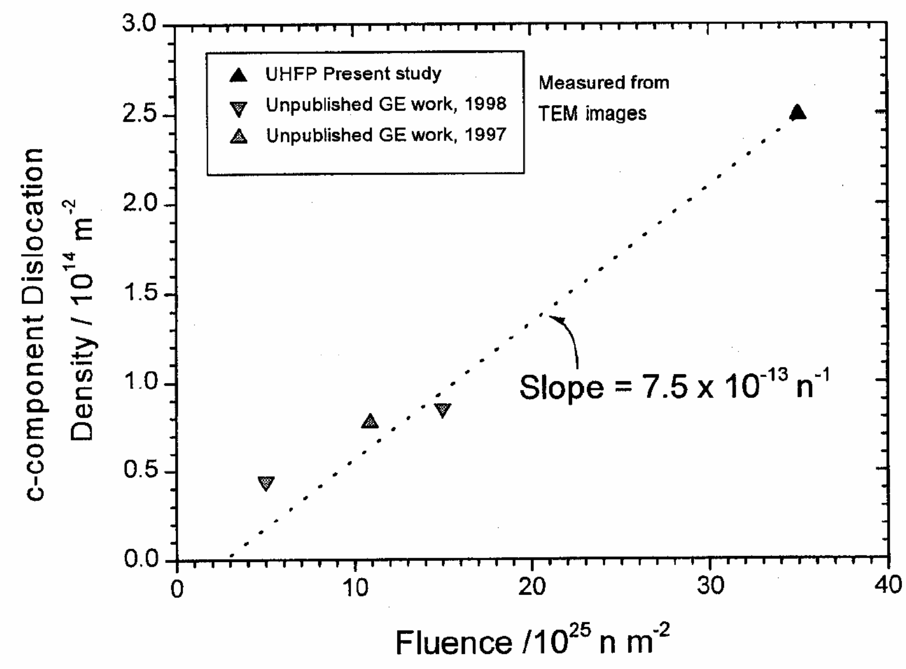

Figure 3-6
Variation of <c> type dislocation density as a function of fluence for Zircaloy-2 irradiated at 290°C (563K) [Mahmood et al., 2000]

3.3 Irradiation Effects on Second-Phase Precipitates

Corrosion resistance in zirconium alloys is intimately related to the presence of second-phase precipitates (SPPs) formed in the zirconium matrix by deliberate additions of alloying elements. The precipitates are usually incoherent crystalline intermetallic compounds, meaning that their physical structure is unrelated to the Zr matrix in which they are imbedded. In as-fabricated Zircaloy-4, the most common SPP is $Zr(Fe,Cr)_2$, while in Zircaloy-2, the most common SPPs are $Zr(Fe,Cr)_2$ and $Zr_2(Fe,Ni)$. For the ZrNb type alloys, the most common SPP is βNb (which is not an intermetallic), and for the ZrSnNbFe type alloys, the most common SPPs are $Zr(Nb,Fe)_2$ and βNb.

At normal light water reactor temperatures [270-370°C (543-643K)], the SPPs change under irradiation in a combination of two ways: amorphization and dissolution.

Amorphization means that the original SPP crystalline structure is converted to an amorphous structure. Amorphization is a complex process, described in some detail by Griffiths et al., 1987; Yang, 1989; Motta, 1997; Bajaj et al., 2002; Taylor et al., 1999; etc. It occurs when an intermetallic compound accumulates enough irradiation-induced defects to cause it to thermodynamically favor an amorphous rather than a crystalline structure.

The rate of amorphization depends on the relative rates of damage creation and damage annealing in the SPP; therefore, important parameters are neutron flux, irradiation temperature, and SPP chemistry. A critical temperature exists above which the annealing processes are fast enough to prevent the damage accumulation of defects needed for transformation. For typical reactor irradiations, amorphization of both $Zr(Fe,Cr)_2$ and $Zr_2(Fe,Ni)$ occurs readily at temperatures near 100°C (373K). At typical LWR temperature [300°C (573K)] and neutron flux, $Zr(Fe,Cr)_2$ becomes amorphous, but $Zr_2(Fe,Ni)$ does not. Above about 330°C (603K), neither SPP becomes amorphous.

The amorphization process begins at the outside surface of the SPP and works its way inward with increasing fluence. This is illustrated in Figure 3-7 [Yang et al., 1986], where the SPP on the left has an amorphous rim (dark area) and the one on the right, at higher fluence, is fully amorphous. There appears to be an incubation period prior to initiation of amorphization, with the incubation fluence decreasing with decreasing temperature in the range 270-330°C (543-603K).

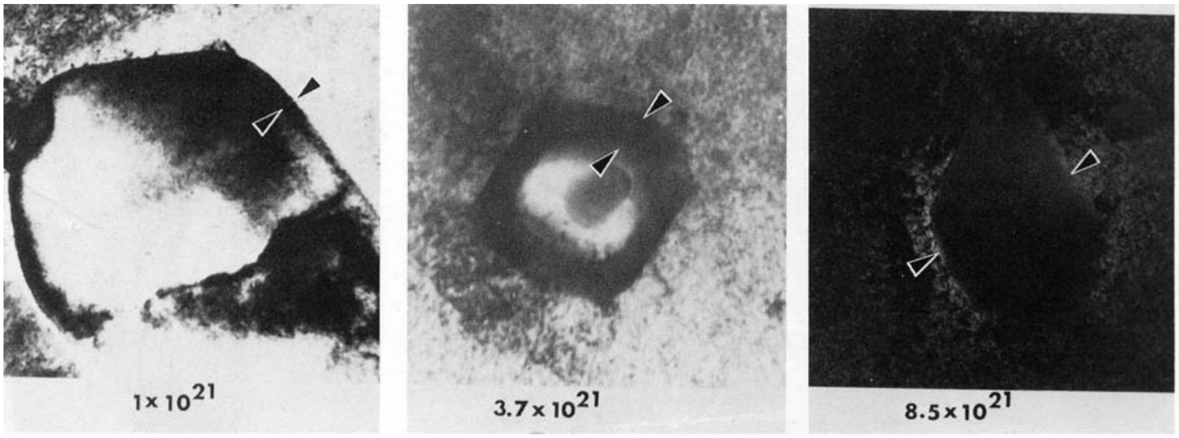

Figure 3-7
Dependence on fluence of the amorphous transformation of $Zr(Fe,Cr)_2$ precipitate in RXA Zircaloy-4, neutron irradiated at 288°C (561K). The arrows indicate the width of the amorphous region [Yang et al., 1986]

Amorphization rate increases as temperature decreases, as neutron flux increases, and as SPP size decreases. Literature evaluation therefore needs to consider reactor and material conditions of specific interest.

The fluence required to produce complete amorphization depends on neutron flux, temperature and SPP size, but for typical $Zr(Fe,Cr)_2$ SPPs of initial size near 0.1 μm, the entire SPP is amorphous by end-of-bundle-life burnups, < 50 MWd/KgU (1×10^{22} n/cm^2, E > 1 MeV).

For the Zr-Nb type alloys, neither the βNb nor $Zr(Nb,Fe)_2$ SPPs become amorphous for irradiation temperature >330°C (603K). However, at 60°C (333K), $Zr(Nb,Fe)_2$ does become amorphous at high fluences.

SPP amorphization in itself does not appear to affect material behavior; however, dissolution of both amorphous and crystalline SPPs does influence corrosion, growth and mechanical properties. At typical LWR operating temperatures, SPP dissolution occurs relentlessly until the SPP essentially disappears.

As SPPs dissolve, the zirconium matrix becomes enriched (well beyond the normal solubility limit) in the dissolving element. For instance in Zircaloy-2, Fe leaves both $Zr(Fe,Cr)_2$ and $Zr_2(Fe,Ni)$ SPPs as schematically illustrated in Figure 3-8 [Mahmood et al., 2000]. This process is described in more detail by Takagawa et al., 2004, Figure 3-9. Here it is seen that Fe rapidly diffuses from the amorphous rim into the matrix, while Cr diffusion is sluggish. At high fluence ($\sim 1 \times 10^{22}$ n/cm^2, E > 1 MeV), complete amorphization and Fe-depletion have occurred, while the Cr level is still high. Only at very high fluence ($\sim 1.5 \times 10^{22}$ n/cm^2, E > 1 MeV) is the Cr dispersed into the matrix, and the SPP essentially disappears.

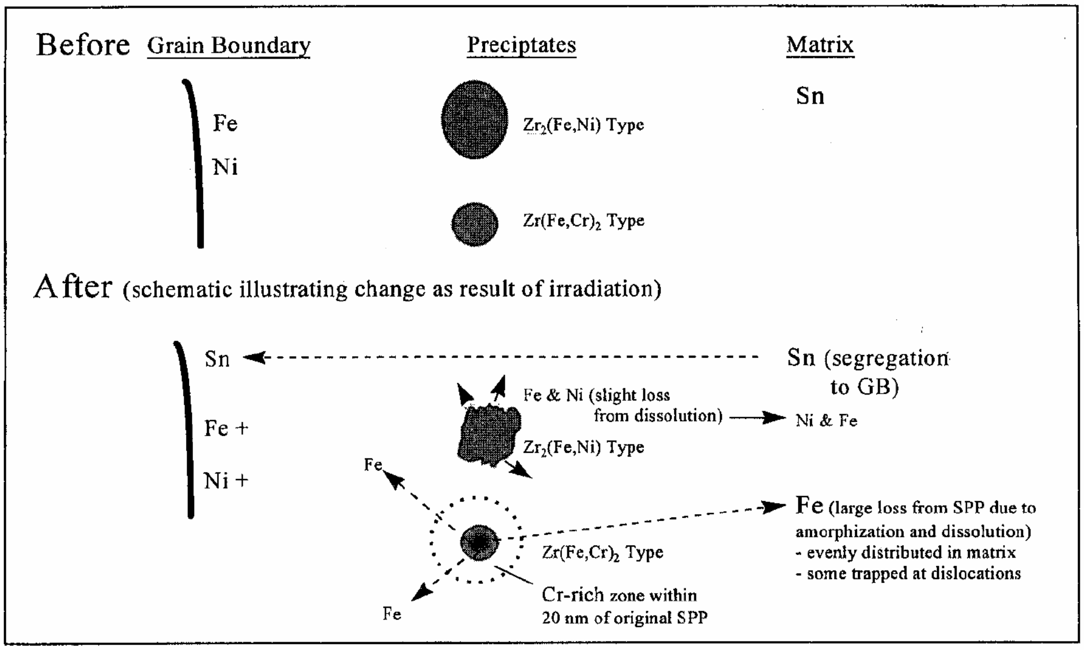

Figure 3-8
Schematic illustrating SPP dissolution and solute redistribution for small SPP in Zircaloy-2 irradiated near 300°C [Mahmood et al., 2000]

The rate of dissolution depends on the SPP size (higher rate for smaller sizes), and the extent of dissolution depends on size and fluence. It has been demonstrated in a BWR that small (< 0.04 µm) SPPs can completely dissolve at low to moderate burnups [Huang et al., 1996]. Also in a PWR, but at temperature near 290°C, SPPs with an average size of 0.2 µm were >80% dissolved at moderate burnup (1×10^{22} n/cm^2, E > 1 MeV) [Garzarolli et al., 2002].

Modelling of the dissolution process gives insight into the alloying concentration of the matrix [Mahmood et al., 1997]. Figure 3-10 illustrates the model for release of solute into the matrix for various size SPPs. For the small SPPs (1R, 2R, 3R), all the Fe is released by moderate burnup.

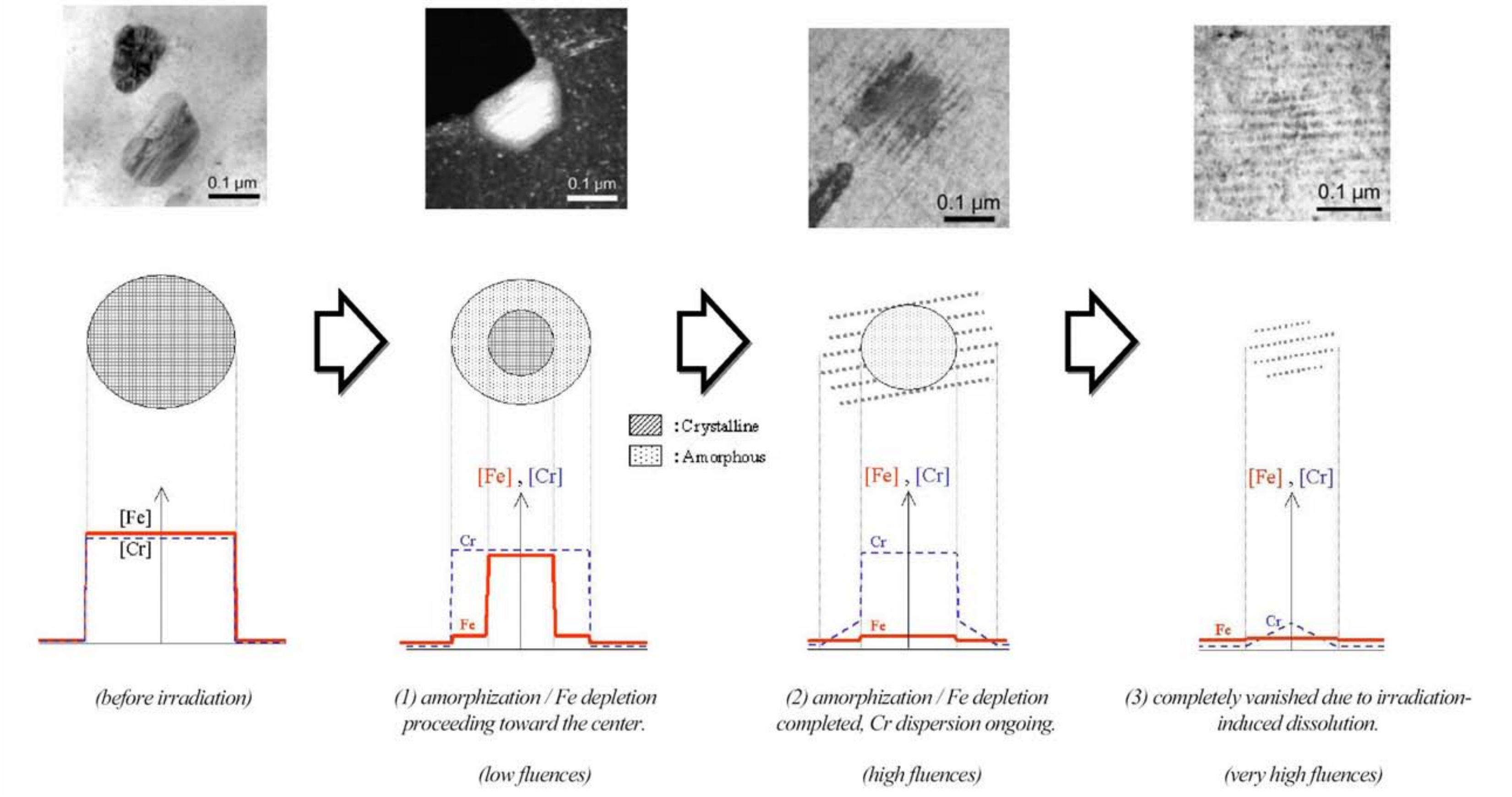

Figure 3-9
Evolution of a Zr-Fe-Cr particle under BWR irradiation. Upper figures: TEM micrographs; middle diagrams: schematic illustration of amorphization; bottom diagrams: schematic illustrations of the chemical compositions [Takagawa et al., 2004]

For the channel material with very large (0.6 µm) SPPs in the unirradiated state, only a small amount of Fe would be released even at high burnups.

In another study, experimental measurement of Fe released from a $Zr(Fe,Nb)_2$ SPP in an E635 alloy containing 0.35% Fe during irradiation at 330-350°C is shown in Figure 3-11 [Shishov et al., 2002]. (In Figure 3-11, fluence has been converted from $E > 0.1$ MeV to $E > 1.0$ MeV by dividing by 4). Here it is seen that the Fe has diffused from the SPP to the alpha Zr matrix such that all of the Fe is in the matrix by moderate burnup. Extending to high burnup (2×10^{22} n/cm^2), in this case, may only increase the probability of re-precipitation of Fe in the matrix. It should be noted that the “normal” solubility of Fe in unirradiated Zr is < 0.02 weight %.

For the Zr-Nb type of alloys the most common SPPs are βNb and $Zr\ (Nb,Fe)_2$. Both are more stable in-reactor than the Zircaloy SPPs, and neither become amorphous at normal PWR temperature. (At 60°C and high burnup, $Zr(Nb,Fe)_2$ does become partially amorphous). However, even at moderate burnup $Zr(Nb,Fe)_2$ loses most of its Fe to the matrix, Figure 3-11, and essentially transforms to a βNb SPP containing 50% Zr and 50% Nb [Shishov et al., 2002] as opposed to the equilibrium form of 13% Zr and 87% Nb.

The interested reader is referred to the literature references for description of the rather intricate details of SPP transformation. It is noted that the SPP changes at high burnup for Zircaloy can be anticipated. For the Zr-Nb type of alloys, the Russian E635 alloy and the French M5 alloy have also been examined at high burnup [Shishov et al., 2005 and Doriet et al., 2005].

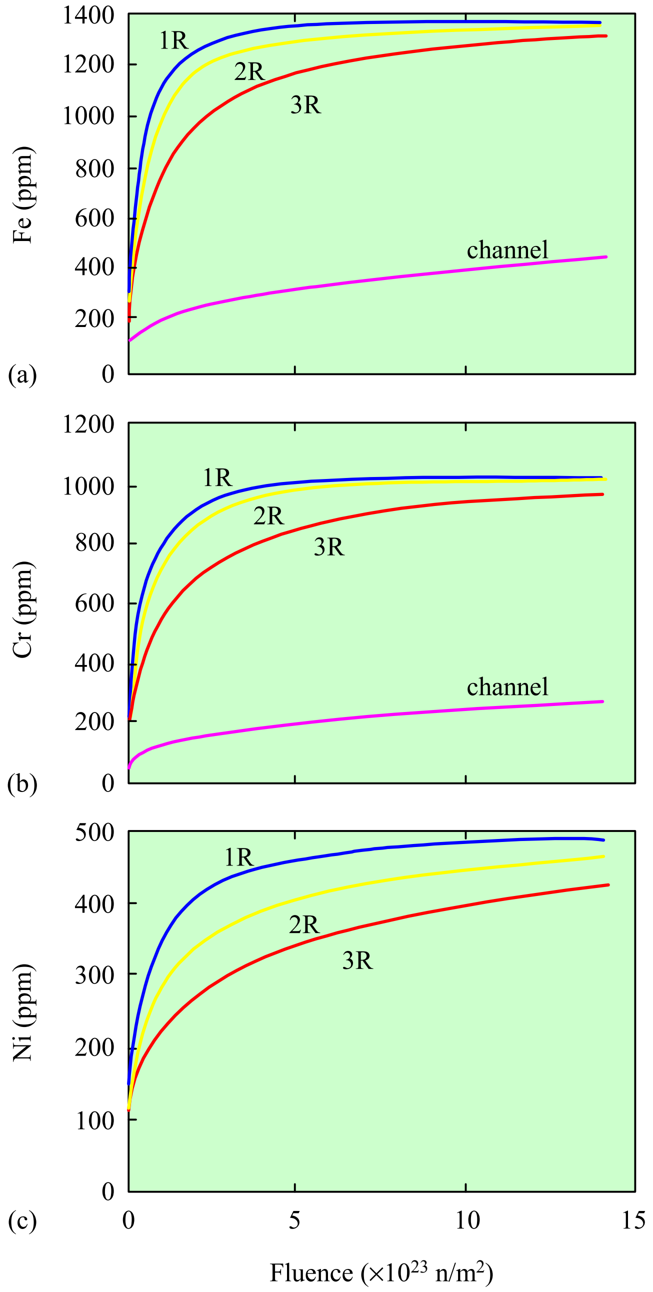

Figure 3-10
Modeling predictions for solute release to the matrix as a function of fluence for Zircaloy-2 (initial SPP size: 1R = 0.026 µm; 2R = 0.042 µm; 3R = 0.056 µm and Zircaloy-4 channel = 0.6 µm) irradiated near 300°C [modified figure according to Mahmood et al., 1997]

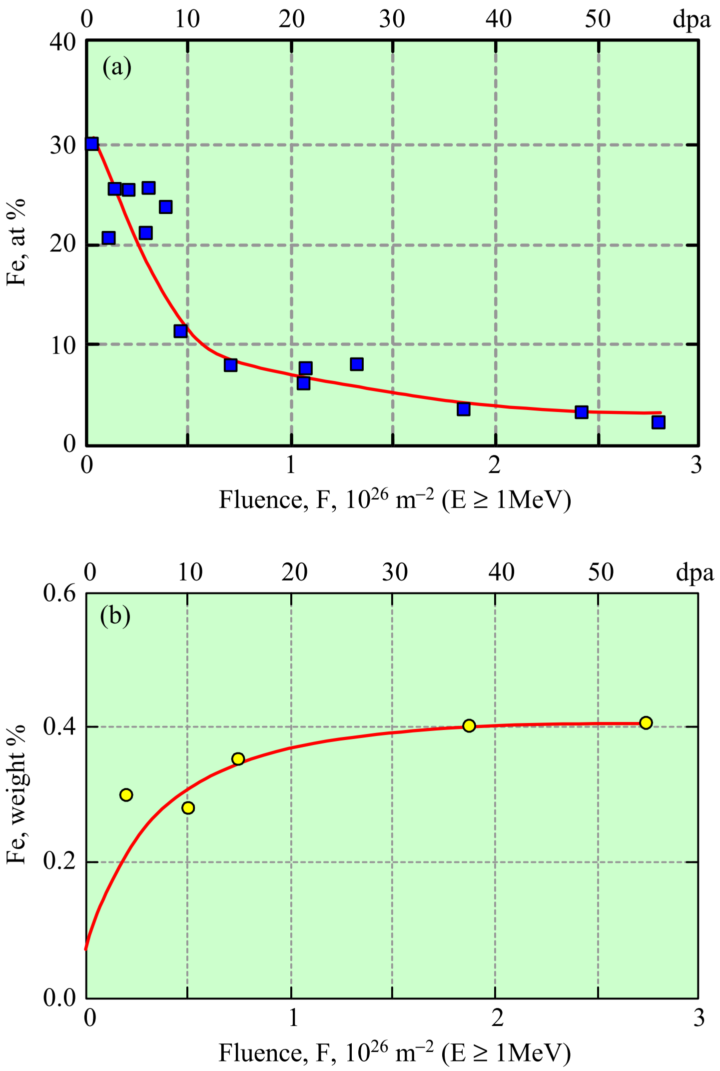

Figure 3-11
Fe content as a function of fluence (E > 0.1 MeV/4) at 330–350°C in alloy E635: (a) SPP Zr(Nb,Fe)$_2$ and (b) –Zr solid solution [modified figure according to Shishov et al., 2002]

4
EFFECTS OF POST-IRRADIATION ANNEALING

4.1 Introduction

Irradiation temperature does have an effect on microstructure. For instance, higher irradiation temperature results in larger <a> loops. <c> loops do not form at 77°C (350K). $Zr_2(Fe,Ni)$ second-phase precipitates (SPPs) do not become amorphous above an irradiation temperature of about 100°C (453K) and $Zr(Fe,Cr)_2$ SPPs do not become amorphous above about 330°C (603K) [e.g., Griffiths et al., 1996]. In addition, post-irradiation temperatures cause effects that give insight to the microstructure stability.

4.2 <a> Loops and Hardness

Damage in the form of <a> loops appears to be stable in post-irradiation annealing conditions to about 400°C (673K). Adamson & Bell, 1986 show that one hour at 400°C is a threshold condition for changes in size and density of <a> loops. Above that temperature, or quite likely a longer time at that temperature, results in a marked increase in loop size and decrease in loop density (see Figure 4-1). Post-irradiation annealing at 550°C (823K) for one hour is sufficient to reduce the loop density to zero. This is accompanied by a dramatic decrease in hardness. Complementary data [Cheng et al., 1994] indicate no changes in <a> loops after 200 days at 316°C (588K).

Kruger, 1990 confirmed the boundaries of the Adamson and Bell data, Table 4-1 and Figure 4-2. The high density of <a> loops formed by a fluence of 3×10^{21} n/cm^2 induced a hardness increase that did not change at the fluence of 12×10^{21} n/cm^2. Post-irradiation annealing at 400°C (673K) for one hour actually resulted in a small increase in hardness, and, at 575°C (848K) or above for one hour, removed both the <a> loops and the hardness increment. Kruger noted that the <a> loop structure was replaced by a loose conglomeration of line dislocations (having an a-component Burgers vector) that did not affect hardness.

Annealing kinetics for the alloy Zr-1%Nb are shown to be similar to Zircaloy by the data of Kobylyansky et al., 2001, in Table 4-2. <a> loop density decreases and size increases rapidly at annealing temperatures above 400°C (673K).

Table 4-1
Characteristics of irradiated and annealed Zircaloy-2. Fluence, 10^{21} n/cm^2 (E > 1 MeV): Low = 3.1; Medium = 8; High = 12. Annealing times are 1 hour [Kruger, 1990]

Condition	**Relative Density**			**<c> Relative Geometry**		**Hardness KHN**[3]
	<a> loops	<a> lines	<c> loops	jogs	size	
Low fluence	high	low	0.1	0	short	250
Medium fluence	high	low	2.9	0	short	-
High fluence	high	low	4.9	0	short	250
High fluence +400°C/1 hr	high	low	4.9	0	short	255
+575°C/1 hr	0	high	3.8	a few	short	180
+625°C/1 hr	0	medium	1.4	some	medium	170
+675°C/1 hr	0	low	0.7	many	long	-
+750°C/1hr	0	0	0	0	0	165

---

[3] KHN = Knoop Hardness Number

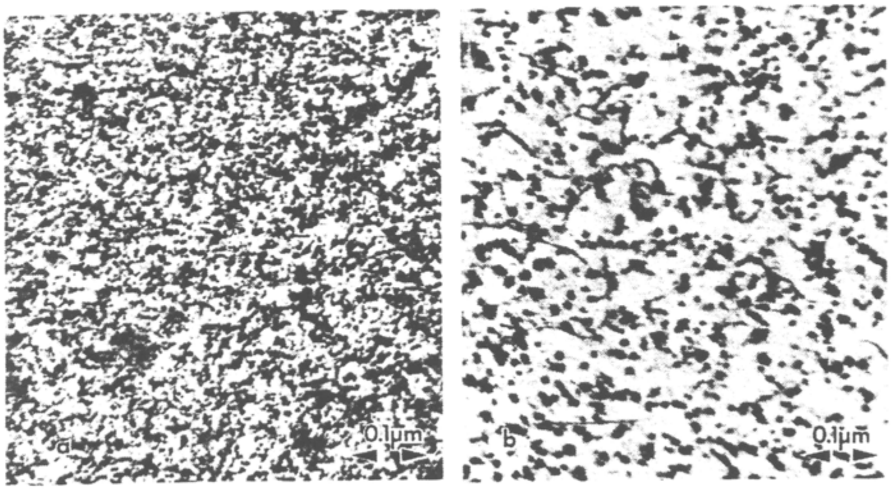

Irradiated Zircaloy, material C, a) 450C, b) 520C.

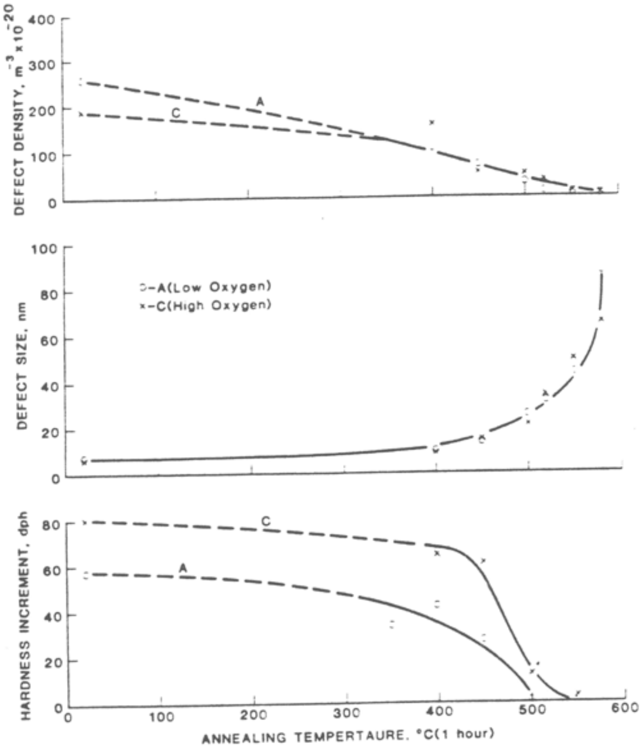

Properties of Zircaloy Irradiated to 6.5×10^{24} n/m^2 (E >1 MeV).

Figure 4-1
Post irradiation microstructure (<a> loop density and size) and hardness of Zircaloy-2 irradiated to a fluence of 6.5 x 10^{20} n/cm^2 (E > 1 MeV). Upper: TEM after annealing at indicated temperatures. Lower: defect density, defect size, and hardness as functions of annealing temperature. Low oxygen (A) is 180 ppm; high oxygen (C) is 1500 ppm [Adamson & Bell, 1986]

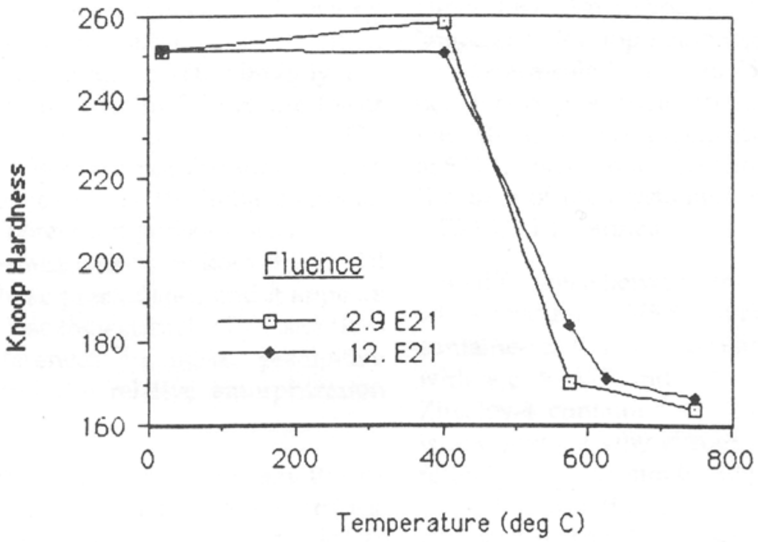

Figure 4-2
Microhardness of irradiated Zircaloy-2 annealed at the indicated temperatures for one hour [Kruger, 1990]

Table 4-2
Zr-1%Nb. Fluence = ~0.5 x 10^{26} m^{-2} (E > 1 MeV). T = ~320°C. Post-annealing time estimated to be two hours

T_{ann} °C	Precipitates			Dislocations (loops and networks)		
	Average size nm	Concentration m^{-3}	Nb Content at.%	Average size nm	Concentration m^{-3}	Density m^{-2}
-	58	1.4 x 10^{8}	52-68	18	2.1 x 10^{10}	-
400	62	1.2 x 10^{8}	55-68	25	1.7 x 10^{10}	-
450	-	1.7 x 10^{8}		160	-	3.1 x 10^{6}
500	63	1.1 x 10^{8}	70-78	230	-	2.9 x 10^{6}

4.3 Hardness Recovery – Fluence Dependence

The early studies of damage annealing behavior were conducted on low fluence materials where the density of <a> loops is still low and not saturated. Those results are not entirely relevant to high burnup fuel, but do give some useful insights. Carpenter and Walters, 1974 used zirconium alloys with fluences of 5 x 10^{19} n/cm^2, E > 0.1 MeV, which converts to about 2.5 x 10^{19} n/cm^2 (E > 1 MeV). Annealing was done for one hour for a number of alloys, instructive ones shown in Table 4-3. At the low fluence, pure zirconium does not irradiation-harden. Zircaloy-2 starts to recover at 300°C (573K), while for Zr-2.5Nb it is 350°C (623K). This indicates that Nb, an important alloying element in modern PWR fuels, does affect the recovery process. It was also noted in Figure 4-1 that Zircaloy with low oxygen (180 ppm) recovered at a lower temperature than normal-oxygen Zircaloy (1500 ppm) [Adamson and Bell, 1986].

Table 4-3
Post-irradiation recovery of Vickers hardness (VHN) for one-hour anneals of various alloys having very low fluence [Carpenter and Walters, 1974]

		Temperature of % recovery, °C	
Alloy	**ΔVHN** (due to irradiation)	**50%**	**100%**
Zirconium	0		
Zircaloy-2	30	380	460
Zr-2.5Nb	45	420	460
Zr-2Ti	50	300	350

On the other hand, Table 4-3 shows that zirconium alloyed with titanium not only hardened more than the other alloys, but it recovered at a lower temperature than the others. So it is seen that impurities or alloying elements do have an influence on damage recovery.

The studies of L. N. Howe, referred to in Douglass, 1971, are often quoted when considering damage annealing. For irradiation at 50°C (323K) to a very low fluence (about 0.3×10^{20} n/cm^2, E > 1 MeV), 50% recovery of the proportional limit (tensile tests) was achieved at 300°C (573K) with full recovery at 400°C (675K) for one-hour anneals. And for irradiation at 280°C (553K) to about 1×10^{20} n/cm^2 (E > 1 MeV), recovery started at 350°C (673K), with 50% recovery at 370°C (643K) and full recovery at 500°C (773K) for one-hour anneals.

Table 4-4 was constructed from data when available under similar experimental conditions. It is clear that low fluence data are not relevant to the cases of high burnup fuel, with fluences sometimes exceeding 100×10^{20} n/cm^2 (E > 1 MeV).

Table 4-4
Thermal recovery of irradiated Zircaloy as a function of fluence x 10^{20} n/cm^2 (E > 1 MeV). Irradiation temperatures near 300°C (573K)

				Recovery, %		
Reference	**Material**	**Fluence**	**Property**	**417°C/1 hr**	**425°C/12 hr**	**512°C/12 hr**
Howe	Zircaloy-2	0.3	Yield	84	-	-
Howe	Zircaloy-2	1	Yield	77	-	-
Adamson & Bell	Zircaloy-2	6	Hardness	16	-	-
	Low-oxygen Zircaloy-2	6	Hardness	63	-	-
Kruger	Zircaloy-2	12	Hardness	0	-	-
Adamson	Zircaloy-4	20	Hardness	8	77	92
Kruger	Zircaloy-2	30	Hardness	3	-	-
Patterson	Zircaloy-4	60	Yield	2	25	77

4.4 Hardness Recovery - Short and Long Times

Torimaru et al., 1996 conducted post-irradiation annealing on RXA Zircaloy-2 having a fluence of 3 x 10^{21} n/cm^2 (E > 1 MeV). They used very high heating and cooling rates to simulate in-reactor transient over-heating. Hardness and tensile properties were measured, and relative irradiation-produced defect density (in this case certainly only <a> loops) was measured by X-ray diffraction techniques. Recovery of defect density and mechanical properties were closely correlated. They found that a treatment of few minutes at 500-550°C (773-823K) or a few seconds at 600-700°C (873-973K) was enough to induce 70-90% recovery, the higher recoveries associated with the higher temperatures.

Ito et al., 2004 report recovery of hardness for Zircaloy at relatively low temperatures and for very long times. De-fueled fuel rod segments were tested for SRA Zircaloy-4 [8 x 10^{21} n/cm^2, E > 1 MeV and T_{irr} about 350°C (623K)] and RXA Zircaloy-2 [(13 x 10^{21} n/cm^2, E > 1 MeV and T_{irr} about 330°C (603K)]. Data are given in Figure 4-3. In Figure 4-3(b), the first few data points are for annealing times of 20, 40, and 150 hours. Hardness measurements are for creep-tested Zircaloy-4 and stress-free Zircaloy-2. Hardness recovery trends are similar to those shown in Figures 4-1 and 4-2 for short times. It is quite significant, however, that hardness recovers for longer times at temperatures as low as 330°C (603K), and for instance nearly 50% recovery occurs for 8,000 hours at 360°C (633K). It is somewhat surprising that full recovery is not attained for long times at 420°C (693K), although the recovery is 80% for either SRA Zircaloy-4 or RXA Zircaloy-2 for 500 hours. This may be related to irradiation temperatures or, in the case of Zircaloy-4, to being measured after creep testing.

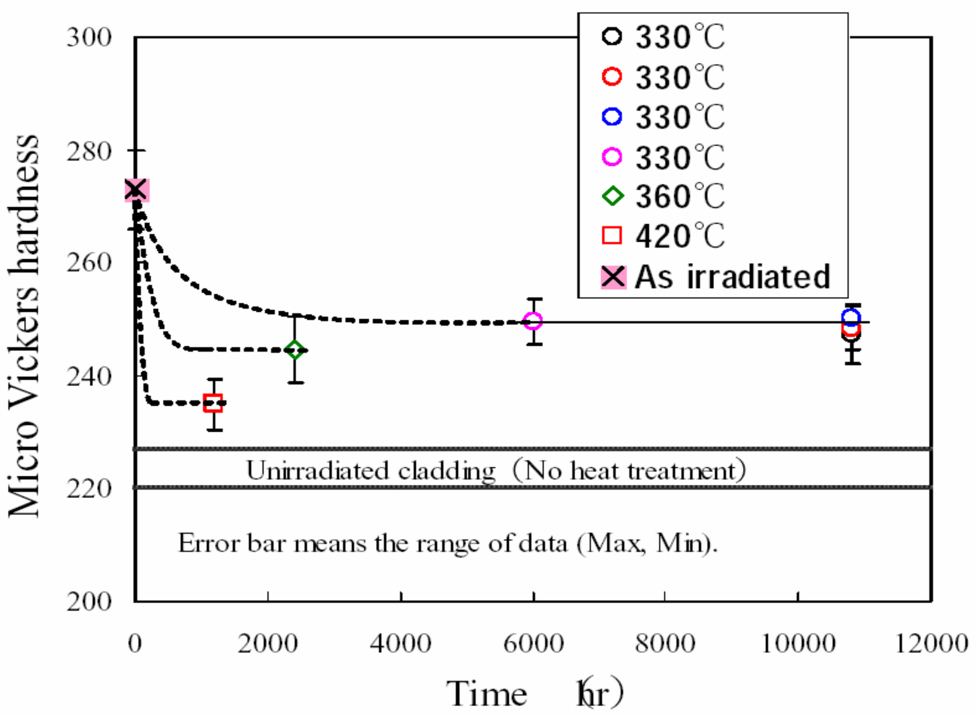

(a) Zry-4 Cladding

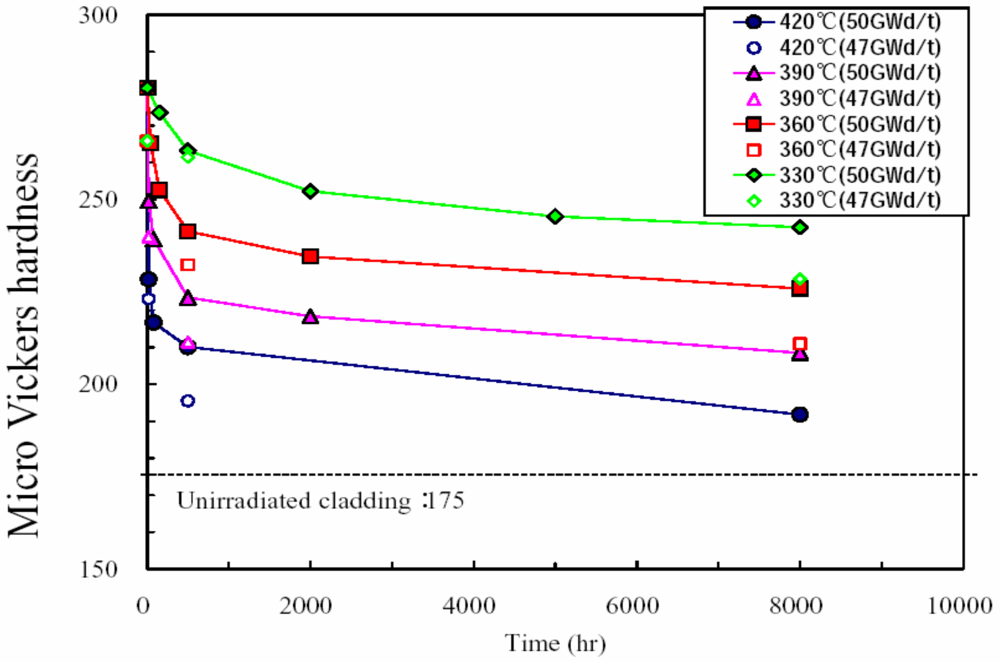

(b) Zry-2 Cladding

Figure 4-3
Recovery of irradiation-induced hardness of SRA Zircaloy-4 and RXA Zircaloy-2 for long times at low temperatures [Ito et al., 2004]

4.5 Recovery of Irradiation Growth

For fluences below the point where <c> loops begin forming, about 3 x 10^{21} n/cm^2 (E > 1 MeV), irradiation growth can be completely recovered by thermal annealing. Since growth in this fluence range is believed to be caused by <a> loops, by anisotropic disposition of zirconium interstitial and vacancies at grain boundaries and perhaps by tiny defect clusters, annealing is relevant to the topic under discussion. Figure 4-4 illustrates growth recovery, as well as yield strength recovery, of RXA Zircaloy-4 irradiated to 2 x 10^{21} n/cm^2 (E > 1 MeV), at about 250°C (523K). For growth, 50% recovery is achieved by five hours at 417°C (690K) or 370°C (643K) for 12 hours.

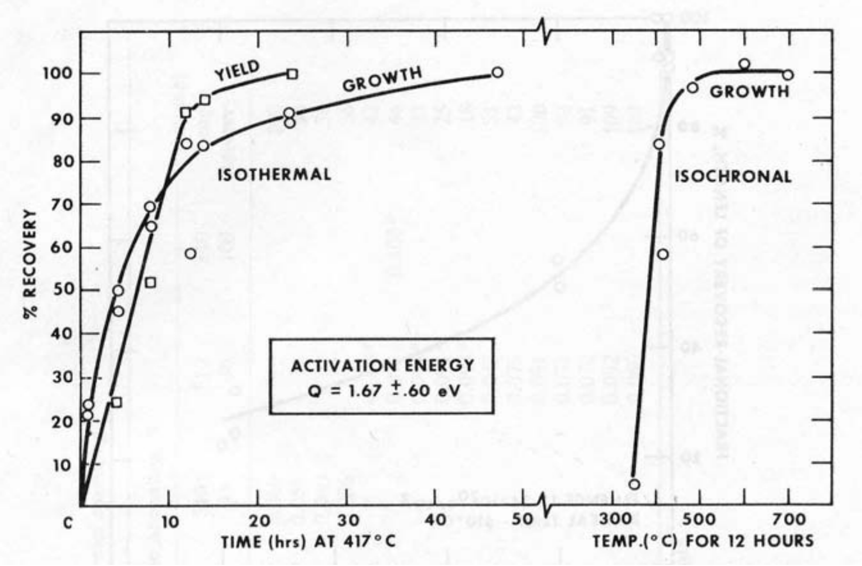

Figure 4-4
Recovery of irradiation growth and yield strength by post-irradiation annealing for various times and temperatures [Adamson, 1977]

4.6 <c> Loop Recovery

On the other hand, <c> component dislocations are quite resistant to change over the whole temperature range where <a> loops disappear. Yang, 1989 and Kruger, 1990 have shown that one hour at 560°C (833K) or 575°C (848K) causes little or no change in <c> loop density or size. One hour at 675°C (948K) results in a > 50% reduction in <c> loop density, while one hour at 750°C (1023K) results in removal of all loops. It was noted that the <c> loops had no effect on hardness. As their density decreased during annealing, they developed jogs (through the climb process) and grew in size. These results were summarized in Table 4-1.

4.7 SPP Recovery

Post-irradiation annealing also has effects on irradiation-affected SPPs. For Zircaloy, Yang, 1989, Kruger, 1990, and Cheng et al., 1994 report that post-irradiation annealing causes SPPs to recrystallize, to re-gain Fe and Ni, and to re-form under specific conditions of time and temperature. Minimal effects are observed for 316°C (589K) for 30 days, but for 200 days significant amounts of Fe diffuse back to the precipitates. At 400°C (673K), Fe diffuses back to precipitates in less than 10 days, and Fe-rich precipitates form at grain boundaries. At higher temperatures, > 560°C (833K), amorphized SPPs recrystallize, Fe and Cr diffuse back to SPPs, and re-precipitation occurs in the matrix and grain boundaries.

Yang, 1989 studied Zircaloy-4 while Kruger, 1990 studied Zircaloy-2, with both works conducted at GE's Vallecitos Nuclear Center. Most behavior was the same for both alloys. However, there was some difference in the effect of annealing on re-precipitation. For Zircaloy-2 (which contains Fe, Cr, and Ni), Fe-Cr-rich and Fe-Ni-rich re-precipitation at grain boundaries occurred at 575°C (848K), and Fe-Cr-rich re-precipitation occurred at grain boundaries at the higher temperatures. For Zircaloy-4 (which has no Ni), only Fe-rich re-precipitation occurred at the lower temperatures, and Fe-Cr re-precipitation occurred only at the highest temperature, 750°C (1023K). This may indicate that Ni in the alloy affects Cr diffusion, or affects the interaction between vacancies and Cr, which is required for Cr diffusion. In addition, diffusion of Fe back into the intragranular precipitates was more sluggish than for Zircaloy-2.

4.8 Summary

Recovery (or annealing) of irradiation effects has many components. Perhaps the most relevant is recovery of irradiation produced <a> and<c> loops; however, defects smaller than these that cannot be "seen" by transmission electron microscopy or X-ray diffraction certainly are important. Indirect evidence of recovery is given by changes in hardness (or mechanical properties) and irradiation growth. Also, although not discussed above, corrosion behaviour can be strongly affected by post-irradiation annealing [Cheng et al., 1994]. Movement of "solute" atoms to and from irradiation-decimated precipitates is an indication that point defects and microchemistry complexes are active.

It is perhaps useful to divide recovery into specific temperature regimes or intervals. It must be noted that in each interval the exact behaviour may be influenced by initial irradiation temperature, amount of cold work, alloy purity or composition, fluence, and, importantly, time scale [e.g., one hour at 400°C (673K) will result in different recovery than one year at 400°C (673K)].

4.8.1 300-400°C (573-673K)

In this regime, fluence, purity, and time are very important. Recovery of hardness can occur in hours in the lower parts of the temperature interval for low fluence or low purity material. For more normal fluence and purity, it is clear that if the annealing temperature is above the irradiation temperature, irradiation-produced defects are starting to move around. Partial hardness recovery can occur at 330-360°C (603-633K) over hundreds or thousands of hours. Fe moves back to SPPs over a few hundred days. Minor reduction of <a> loop density and hardness occurs. Irradiation growth starts to recover. In this regime recovery is sluggish, but is occurring. However, one should be careful not to use the results obtained for very low fluence materials as representative of high fluence material.

4.8.2 400-500°C (673-773K)

It is clear that in this regime defect annealing is well underway. Hardness and irradiation growth recovers rapidly and may be complete by 500°C (673K) in a few hours. Density of <a> loops is rapidly decreasing. Fe diffuses back to SPPs in a few days. On the other hand, no significant changes occur in <c> loops or grain size.

4.8.3 500-600°C (773-873K)

In this regime <a> loops disappear altogether and are replaced by a loose network of line dislocations. Hardness recovers completely, needing only a few minutes at > 500°C (773K). In Zircaloy-2, Fe and Cr move rapidly to grain boundaries and SPPs, while in Zircaloy-4 only Fe does the same. A few jogs are forming on <c> loops, indicating a movement of vacancies to the loop edges, but only minor decrease in <c> loop density occurs.

4.8.4 600-700°C (873-973K)

In this regime hardness increments and loops are gone, even after a few seconds at temperature. For both Zircaloy-2 and -4, Cr is diffusing to grain boundaries and SPPs. <c> loop density is decreasing and the c-component segments are becoming long and heavily jogged.

4.8.5 700-750°C (973-1023K)

In this regime, a few minutes are enough to remove all <c> loops and a-line dislocations. Structure appears similar to unirradiated material. Intergranular SPPs are absent, and intragranular SPPs are recrystallized and larger than in the initial unirradiated condition.

5

POSSIBLE SYNERGIES BETWEEN DAMAGE ANNEALING, HYDROGEN SOLUBILITY, AND DRY STORAGE AND TRANSPORTATION

An important issue in the evaluation of spent fuel cladding integrity during storage and transportation is the effect of hydrides on cladding resistance to failure. At issue are the consequences of loading challenges such as accidental impact during handling, cask tip-over, or accidental drop during transportation. The degree to which spent fuel cladding, after a number of years in dry storage, could retain sufficient strength and ductility to resist catastrophic failures under these loading challenges would strongly depend on the spatial distribution and orientation of the hydrides.

At the end of its useful life, spent fuel is initially stored in the spent fuel pool; the hydrogen in the cladding is predominantly in the form of circumferentially oriented zirconium hydride platelets. This hydride morphology is the consequence of hydrogen uptake during the slow in-reactor corrosion process, and results in significant, but operationally tolerable, changes in the cladding mechanical properties. When spent fuel is transferred out of wet storage and placed into a dry storage system, cladding temperatures increase and reach their highest levels either during fuel loading operations (e.g., during vacuum drying), or shortly thereafter during the early stages of dry storage. Peak cladding temperatures dictate how many hydrides can potentially re-dissolve, and, consequently, how much hydrogen goes back into solid solution in the Zircaloy matrix. In the U.S., peak cladding temperatures are bounded by the regulatory limit of 400°C for normal conditions of storage [NRC, 2003]. This temperature limit effectively determines the maximum amount of hydrogen that will eventually re-precipitate back in the form of zirconium hydrides as the cladding slowly cools down during interim dry storage. At a temperature of 400°C, the maximum amount of hydrogen in solid solution in unirradiated Zircaloy cladding is ~200 ppm. Upon cooling, hydrogen may re-precipitate in the form of circumferential hydrides, radial hydrides, or both, depending on the magnitude of cladding hoop stress, with radial hydrides having the greater deleterious effects on cladding behavior. The precipitation rate and the concentration fractions of precipitating radial and circumferential hydrides depend on the initial magnitudes and the time histories of temperature and stress during storage (Rashid and Machiels, 2005).

Only hydrides that are dissolved and then re-precipitated over time during dry storage can potentially re-orient. Local cladding temperatures control how many hydrides dissolve, and consequently the amount of hydrogen going back into solid solution in the Zircaloy matrix, as determined by the terminal solid solubility of hydrogen upon heating (solution), or TSSs. Upon cooling, re-precipitation of hydrogen in the form of hydrides will begin at a substantially lower temperature, as determined by the terminal solid solubility of hydrogen upon cooling (precipitation), or TSSp.

As discussed in the previous sections, it is likely that hydrogen atoms interact with irradiation-produced <a> and <c> dislocation loops and/or with Fe or Cr "solutes" driven from second-phase precipitates (SPPs) during irradiation. The amount of hydrogen in this category appears to be in the range 25-200 ppm, as determined by the few studies of this phenomenon, summarized in Section 2. This "trapped" hydrogen cannot be classified as either "soluble hydrogen" or "hydrides" at any particular temperature. As a consequence, trapped hydrogen does not participate in the "classic dissolution/precipitation process" governed by the TSSs and TSSp curves. Given that only hydride that is dissolved can potentially re-orient, hydrogen trapping can be beneficial in terms of limiting the amount of hydrogen going back in solution when cladding temperatures increase upon transfer of the spent fuel from wet to dry storage. This would be the case when the fraction of hydrogen in the form of hydrides is lower than that needed to achieve the solubility limit given by the TSSs curve. However, depending on the cladding thermal history during storage, trapped hydrogen could also be incrementally released to the zirconium matrix when trapping defects are eliminated by thermal annealing. Such a time-delayed release of hydrogen could, potentially, result in enhanced precipitation of radially oriented hydrides, which would be an undesirable outcome.

Without knowing which traps are most effective and are most stable during dry storage, it is difficult to predict how much hydrogen can be released. The hydrogen solubility data of both McMinn et al., 2000 and Vizcaino et al., 2002 and 2005 indicate that release of trapped hydrogen occurs in the temperature ranges where irradiation damage is also recovering (annealing), although it is not possible with currently available data to firmly associate the hydrogen trapping to specific defects:

- In the cases where <c> loops do *not* exist in substantial numbers, it appears that trapped hydrogen can be completely, or almost completely, released at temperatures at which most or all <a> loops should be eliminated and at which Fe is at least sluggishly mobile in the lattice. For instance, McMinn reported only partial recovery for 400°C (673K)/1 hour, but full recovery for 500°C (773K)/1 hour, and Table 2-1 indicates that Vizcaino's 4 x 10^{21} n/cm^2 material releases most of the trapped hydrogen for long anneals at 611°C (884K) or 508°C (781K).
- In cases where <c> loops do exist, it appears that higher temperature anneals are required for complete recovery. McMinn's 1 x 10^{22} n/cm^2 material has only 60% recovery at 500°C (773K)/1 hr., when all <a> loops, but no <c> loops, should be gone. Likewise, Vizcaino's 7-9 x 10^{21} n/cm^2 materials recover by <75% for very long times at 611°C (884K) and <50% at 508°C/2 hours. Since <c> loop annealing does not become rapid until at least 625°C (898K), it appears that there may be a <c> loop-H interaction. Or perhaps there is a Cr-H interaction, as Cr becomes mobile in the same temperature ranges.

If the temperatures are in the 500-400°C (773-673K) range (see "French" transportation scenario in Section 1), it is likely that all the <a> loops and a very small fraction of <c> loops will disappear and much dissolved Fe will be reabsorbed by the SPPs. In that case, if it is assumed that the traps are not saturated it is likely that the amount of H released will be proportional to or at least related to the total amount of H absorbed during the corrosion process. Assuming that the time required for annealing a substantial fraction of the irradiation traps is long compared to the time required for establishing the equilibrium hydride/dissolved hydrogen concentration in the cladding and that cladding hoop stresses are greater than the "threshold" stress[4], a fraction of the H released from traps is likely to eventually re-precipitate in the radial orientation. For instance, at 400°C (673K) one would normally expect no more than about 200 ppm H in solution.[5] If the total hydrogen is 500 ppm, then about 300 ppm hydride would normally remain in the circumferential orientation at 400°C (673K) if no trapping occurred, and 200 ppm of hydrogen would be in play for potential re-orientation. But if 100 ppm hydrogen were trapped and then released, there would be only 200 ppm of hydrogen remaining as circumferential hydrides, and up to 300 ppm of hydrogen could eventually be in play for potential re-orientation. Annealing temperatures in the 500-400°C (773-673K) range are not likely to affect <c> loops, although the influence of very long times is not known. Although the relative trapping strengths of <a> and <c> loops is not known, available data indicate the <c> loop is a deeper (stronger) trap.

If the initial storage temperatures are in the 400-300°C (673-573K) range ("US" scenario in Section 1), it is almost certain that <c> loops will not be a factor in releasing hydrogen. For very long times, it can be assumed that <a> loops and SPP/solute annealing will occur. The data of McMinn et al. indicate that about 40% of the trapping occurs by <c> loops, or other phenomenon stable at >500°C (773K). This could be used as a rough guide, but will depend on the dynamics and timing of loop and hydrogen creation. If most of the corrosion occurs before <c> loops form, which is before ~15 GWd/MT burnup (see Section 3.2), then most of the trapped H will be in <a> loops. If the corrosion occurs at higher burnups, some of the hydrogen will be trapped in <c> loops.

Another complication is that different alloys will very likely trap hydrogen in different ways. Alloys such as M5™ and ZIRLO™ may not form <c> loops at all. The density of <a> loops may be similar for all alloys, but the trapping strength of the <a> loops may be altered, for instance, by interactions between Nb and O with the loops.

---

[4] Defined as the stress at which some limited amount of re-orientation is observed.

[5] The terminal solid solubility for solution, TSSs, is about 200 ppm H.

6

MISSING DATA AND POTENTIAL ADDITIONAL WORK

One of the problems in using the literature recovery data is that the kinetics of recovery or annealing has not been quantified. It is not known, for instance, how strongly recovery depends on time at temperature. How different is 380°C (653K) for 1 hour and 380°C (653K) for 1000 hours? If a simple chemical rate (Arrhenius) equation applies, then recovery (R), time (t) and temperature (T) can be related:

$$R = Kte^{-Q/RT}$$

Appropriate activation energies and constants can be derived from results of isochronal and isothermal anneals, such as those shown for irradiation growth in Figure 4-4. Then, results of any combination of t and T could be calculated. The problem with this approach is that the activation energy, Q, of the Arrhenius reaction is not really a constant. In the case of the recoveries of hardness or growth and, particularly, hydrogen solubility, there are several recovery processes that act in different temperature regions; therefore, a single activation energy cannot describe recovery over more than about a 50°C (50K) temperature range. Nevertheless a useful experiment, if H-solubility is related to the existence of <a> and <c> loops, would be to conduct careful TEM or X-ray diffraction examinations on the size and density of these defects in temperature regions of interest for long term storage issues. Similar studies could be conducted on hardness recovery, which is directly related to the presence of <a> loops.[6] Such studies should be done on material irradiated to appropriate fluences and on alloys of specific interest.

Another area that is not understood is the actual interaction between hydrogen and the <a> and <c> loops and between hydrogen and the irradiation-produced "solutes" Fe, Cr and Ni. It is likely that this type of work would need to be done by modeling and calculation, supplemented by microstructure studies. Possible approaches include the molecular dynamics computations of the type described by Hayoshi, et al., 2005, the "ab initio" modeling of the type described by Ferrer, et al., 2002, and/or the nuclear microanalysis work of Lewis, 1984.

Although on the periphery of the current topic, another area of interest is the effect of Fe on diffusion in the zirconium matrix. It could well be that the behavior of hydrogen is affected by such diffusion phenomena. A reference is King et al., 1991.

Metallographic examinations of hydride distributions in the irradiated material have always been conducted at room temperature. To gain more understanding of the balance between hydrides in

---

[6] It should be noted that hardness in irradiated material is related more closely to the ultimate tensile strength rather than the yield stress.

radial and circumferential orientations and hydrogen in solution, hot-stage metallography would be useful. None has been reported so far.

Of course, the data of McMinn et al., 2000 and Vizcaino et al., 2002 are crucial. Examination and extension of their data and analysis, including detailed TEM microstructure examinations of their materials would be very useful.

7
REFERENCES

Adamson, R. B., "*Irradiation Growth of Zircaloy", Zirconium in the Nuclear Industry; Third Conference*, ASTM STP 633, pp. 326, ASTM, 1977.

Adamson, R. B. and W. L. Bell, "*Effects of Neutron Irradiation and Oxygen Content on the Microstructure and Mechanical Properties of Zircaloy*", Microstructure and Mechanical Behavior of Materials, Proceedings: Int'l Symposiums, Xian, China, Oct. 1985, EMAS, Warley, UK, 237-246, 1986.

Adamson, R. B., "*Effects of Neutron Irradiation on Microstructure and Properties of Zircaloy*", Zirconium in the Nuclear Industry; Twelfth International Symposium, ASTM STP 1354, ASTM, pp. 15-31, West Conshohocken, PA, 2000.

Bajaj, R., B. F. Kammenzind, and D. M. Farkas., *"Effects of Neutron Irradiation on the Microstructure of Alpha-Annealed Zircaloy-4*", Zirconium in the Nuclear Industry: 13th International Symposium, ASTM STP 1423, G. D. Moan and P. Rudling, Eds., ASTM International, West Conshohocken, PA, pp. 400-426, 2002.

Carpenter, G.J.C. and J. F. Watters, *"Irradiation Damage Recovery in Some Zirconium Alloys", Zirconium in Nuclear Applications,* ASTM STP 551, ASTM, pp.400-415, 1974.

Cheng, B-C., R. M. Kruger, and R. B. Adamson, "*Corrosion Behaviour of Irradiated Zircaloy*", Proc. 10th Int. Symp. in the Nucl. Ind., ASTM-STP-1245, pp. 400-418, 1994.

Davies, P. H., R. R. Hosbons, M. Griffiths, and C. K. Chow, "*Correlation Between Irradiated and Unirradiated Fracture Toughness of Zr-2.5Nb Pressure Tubes*", Zirconium in the Nuclear Industry: Tenth International Symposium, ASTM STP 1245, A. M. Garde and E. R. Bradley, Eds., American Society for Testing and Materials, Philadelphia, 135-167, 1994.

Doriot, S., D. Gilbon, J.-L. Béchade, M.-H. Mathon, L. Legras, and J.-P. Mardon, "*Microstructural Stability of M5™ Alloy Irradiated up to High Neutron Fluences*", Proc: 14th Int. ASTM Symposium on Zr Alloys in Nuclear Industry, Stockholm, 2004.

Franklin, D. G., G. E. Lucas G. E., and A. L. Bement, "*Creep of Zirconium Alloys in Nuclear Reactors*", ASTM Special Technical Publication 815, American Society for Testing and Materials, 1983.

Ferrer, F., A. Barbu, T. Bretheau, J. Crepin, F. Willaime, and D. Charquet, "*The Effect of Small Concentrations of Sulfur on the Plasticity of Zirconium Alloys at Intermediate Temperatures",* Zirconium in the Nuclear Industry: 13th Int'l Symposium, ASTM STP 1423, G. D. Moan and P. Rudling, Eds., American Society for Testing and Materials, pp. 863-887, 2002.

Griffiths, M., R. W. Gilbert, and C. J. C. Carpenter., "*Phase Instability, Decomposition and Redistribution of Intermetallic Precipitates in Zircaloy-2 and -4 During Neutron Irradiation*", Journal of Nuclear Materials, Vol. 150, pp. 53-66, North-Holland, Amsterdam, 1987.

Griffiths, M., J. F. Mecke, and J. E. Winegar, "*Evolution of Microstructure in Zirconium Alloys During Irradiation*", Zirconium in the Nuclear Industry: 11th Int'l Symposium, ASTM STP 1295, E. R. Bradley and G. P. Sabol, Eds., American Society for Testing and Materials, 580-602, 1996.

Griffiths, M., R. A. Holt, and A. Rogerson, "*Microstructural aspects of accelerated deformation of Zircaloy nuclear reactor components during service*", J. Nucl. Mat. 225, pp. 245-258, 1995.

Hayashi, H., K. Ogata, T. Baba, and K. Kamimura, *"Understanding Irradiation and Hydride Embrittlement of Cladding by the Computational Science"*, paper 1.5, IAEA Technical Meeting on Fuel Behavior Modelling under Normal, Transient, and Accident Conditions and High Burnups, Kendal, United Kingdom, September, 2005.

Howe, L.M., in Douglass, D.L., *The Metallurgy of Zirconium"*, Supplement 1991, International Atomic Energy Agency, pp. 313-320, 1971.

Ito, K., K. Kamimura, and Y. Tsukuda, *"Evaluation of irradiation effect on spent fuel cladding creep properties",* Proceedings of the 2004 International Meeting on LWR Fuel Performance, Paper 1117, Orlando, Florida, Sept.19–22, 2004.

King, A. D., G. M. Hood, and R. A. Holt, *"Fe-enhancement of self-diffusion in alpha-Zr",* J. Nuclear Materials **185,** pp 174-181, 1991.

King, S. J., R. L. Kesterson, K. H. Yueh, R. J. Comstock, W. M. Herwig, and S. D. Ferguson, "*Impact of Hydrogen on Dimensional Stability of ZIRLO ™ Fuel Assemblies*", ASTM "13th Int'l Conference on Zirconium in the Nuclear Industry", Annecy, France, June 10-14, ASTM STP 1423, pp. 471-489, 2002.

Kobylyansky, G.P, V. K. Shamardin, and Z. E. Ostrovsky, *"Effect of temperature factors on irradiation-induced growth of zirconium alloys at high neutron fluences"*, poster, 13th ASTM Symposium in Annecy, 2001.

Kruger, R.M., *"Precipitate Stability in Zircaloy-2"*, EPRI NP-6845-D, 1990.

Lewis, M.B., *"Deuterium-Defect Trapping in Ion-Irradiated Zirconium",* Journal of Nuclear Materials 125, pp. 152-159, 1984.

Mahmood, S. T., K. W. Edsinger, D. M. Farkas, and R. B. Adamson, "*Effects of SPP Dissolution on Mechanical Properties of Zircaloy-2*", Proc., Int. Topical Meeting on LWR Fuel Performance, ANS, Portland, pp. 440-451, March 2-6, 1997.

Machiels, A., private communication, EPRI, 2006.

Mahmood, S. T., D. M. Farkas, and R. B. Adamson, "*Post irradiation characterization of ultra-high-fluence Zircaloy-2 plate*", Zirconium in the Nuclear Industry; Twelfth International Symposium, ASTM STP 1354, ASTM, pp. 139-169, West Conshohocken, PA, 2000.

McMinn, A., E. C. Darby, and J. S. Schofield, "*The Terminal Solubility of Hydrogen in Zirconium*", Proc. 12th Int. Symp. on Zr in the Nucl. Ind., ASTM-STP-1354, pp. 173-195, 2000.

Motta, A., "*Amorphization of Intermetallic Compounds under Irradiation – A Review*" Journal of Nuclear Materials, Vol. 244, pp. 227-250, 1997.

NRC, Interim Staff Guidance – 11, *"Cladding Considerations for the Transportation and Storage of Spent Fuel"*, Revision 3, November 2003.

Patterson, P.W., WAPD-FD(RMH)-B19, 1970.

Rashid, J. Y. R. and A. J. Machiels, *"Hydride Precipitation in Spent Fuel Cladding during Storage and Consequent Effects on Fuel Integrity"* 10th International Conference on Environmental Remediation and Radioactive Waste Management, Glasgow, Scotland, September 4-8, 2005.

Roy, C., *"Nucleation of Hydrides in Zirconium Alloys",* Atomic Energy of Canada Ltd., Report AECL-2297, 1965.

Shaltiel, D., I. Jacob, and D. J. Davidov, J. Less-Common Metals 53, p.117, 1977.

Shishov, V. N., M. M. Peregud, A. V. Nikulina, P. V. Shebaldov, A. V. Tselischev, A. E. Novoselov, G. P. Kobylyansky, Z. E. Ostrovsky, and V. K. Shamardin, *"Influence of Zirconium Alloy Chemical Composition on Microstructure Formation and Irradiation Induced Growth",* Zirconium in the Nuclear Industry: 13th Int'l Symposium, ASTM STP 1423, G. D. Moan and P. Rudling, Eds., American Society for Testing and Materials, pp. 758-779, 2002.

Shishov, V. N., M. M. Peregud, A. V. Nikulina, G. P. Kobylyansky, A. E. Novoselov, Z. E. Ostrovsky, A. V. Obukhov, and Y. V. Pimenov, "*Influence of Structure and Phase State on Irradiation Induced Growth of Niobium Containing Alloys of Zirconium*", Proc. 14th ASTM Symposium on Zirconium in the Nuclear Industry, Stockholm, 2005.

Takagawa, Y., S. Ishimoto, Y. Etoh, T. Kubo, K. Ogata, and O. Kubota, "*The Correlation between Microstructures and in-BWR Corrosion Behavior of Highly Irradiated Zr-based Alloys*", Proc. 14th ASTM Symposium on Zirconium in the Nuclear Industry, Stockholm, 2004.

Taylor, D. F., H. R. Peters, and W. J. S. Yang, "*Amorphization of Laves-Phase Precipitates in Zircaloy-4 by Neutron Irradiation*", in Proceedings of the 9th International Conference on Environmental Degradation of Materials in Nuclear Power Systems-Water Rectors (TMS), August, 1999.

Torimaru, T., T. Yasuda, and M. Nakatsuka, "*Changes in mechanical properties of irradiated Zircaloy-2 fuel cladding due to short term annealing*", Journal of Nuclear Materials 238, 169-174, 1996.

Vizcaino, P., A. D. Banchik, and J. P. Abriata, "*Solubility of Hydrogen in Zircaloy-4: Irradiation Induced Increase Thermal Recovery*", J. Nucl. Mater., 304, pp. 96-106, 2002.

Vizcaino, P., D. R. Bianchi, R. O. Rios, A. D. Banchik, and J. P. Abriata, "*Effect of Post Irradiation Thermal Treatment On The Crystalline Structure of the Zircaloy-4 Cooling Channels of the PHWR Atucha I",* TM-Argentina-2005, Technical Meeting on "Behavior of High Corrosion Resistance Zr-based Alloys", Buenos Aires, 23-28 October, 2005.

Yang, W. J. S., R. P. Tucker, B. Cheng, and R. B. Adamson, "*Precipitates in Zircaloy: Identification and the Effects on Irradiation and Thermal Treatment*", Journal of Nuclear Materials, Vol. 138, pp. 185-195, North-Holland, Amsterdam, 1986.

Yang, W. J. S., "*Microstructural Development in Neutron Irradiated Zircaloy-4*", Effects of Radiation on Materials: 14th Int'l Symposium, Vol. 1, ASTM STP 1046, N. H. Packan, R. E. Stoller, and A. S. Kumar, Eds., American Society for Testing and Materials, Philadelphia, 442-456, 1989.

WARNING: This Document contains information classified under U.S. Export Control regulations as restricted from export outside the United States. You are under an obligation to ensure that you have a legal right to obtain access to this information and to ensure that you obtain an export license prior to any re-export of this information. Special restrictions apply to access by anyone that is not a United States citizen or a permanent United States resident. For further information regarding your obligations, please see the information contained below in the section titled "Export Control Restrictions."

Export Control Restrictions

Access to and use of EPRI Intellectual Property is granted with the specific understanding and requirement that responsibility for ensuring full compliance with all applicable U.S. and foreign export laws and regulations is being undertaken by you and your company. This includes an obligation to ensure that any individual receiving access hereunder who is not a U.S. citizen or permanent U.S. resident is permitted access under applicable U.S. and foreign export laws and regulations. In the event you are uncertain whether you or your company may lawfully obtain access to this EPRI Intellectual Property, you acknowledge that it is your obligation to consult with your company's legal counsel to determine whether this access is lawful. Although EPRI may make available on a case-by-case basis an informal assessment of the applicable U.S. export classification for specific EPRI Intellectual Property, you and your company acknowledge that this assessment is solely for informational purposes and not for reliance purposes. You and your company acknowledge that it is still the obligation of you and your company to make your own assessment of the applicable U.S. export classification and ensure compliance accordingly. You and your company understand and acknowledge your obligations to make a prompt report to EPRI and the appropriate authorities regarding any access to or use of EPRI Intellectual Property hereunder that may be in violation of applicable U.S. or foreign export laws or regulations.

Printed on recycled paper in the United States of America

The Electric Power Research Institute (EPRI)

The Electric Power Research Institute (EPRI), with major locations in Palo Alto, California, and Charlotte, North Carolina, was established in 1973 as an independent, nonprofit center for public interest energy and environmental research. EPRI brings together members, participants, the Institute's scientists and engineers, and other leading experts to work collaboratively on solutions to the challenges of electric power. These solutions span nearly every area of electricity generation, delivery, and use, including health, safety, and environment. EPRI's members represent over 90% of the electricity generated in the United States. International participation represents nearly 15% of EPRI's total research, development, and demonstration program.

Together...Shaping the Future of Electricity

Program:
Nuclear Power

1013446

ELECTRIC POWER RESEARCH INSTITUTE
3420 Hillview Avenue, Palo Alto, California 94304-1395 • PO Box 10412, Palo Alto, California 94303-0813 USA
800.313.3774 • 650.855.2121 • askepri@epri.com • www.epri.com